# Electron Paramagnetic Resonance Spectroscopic Characterization of Dimethyl Sulfoxide Reductase of *Escherichia coli*†

Richard Cammack*,‡ and Joel H. Weiner§

*Department of Biochemistry, University of Alberta, Edmonton, Alberta, Canada T6G 2H7, and Division of Biomolecular Sciences, Biochemistry Section, King's College, London, Campden Hill Road, London W8 7AH, U.K.*

*Received October 24, 1989; Revised Manuscript Received May 24, 1990*

ABSTRACT: The electron transfer centers in dimethyl sulfoxide reductase were examined by EPR spectroscopy in membranes of the overproducing *Escherichia coli* strain HB101/pDMS159, and in purified enzyme. Iron–sulfur clusters of the [4Fe–4S] type and a molybdenum center were detected in the protein, which comprises three different subunits: DmsA, -B, and -C. The intensity of the reduced iron–sulfur clusters corresponded to 3.82 ± 0.5 spins per molecule. The dithionite-reduced clusters were reoxidized by DMSO or TMAO. The enzyme, as prepared, showed a spectrum of Mo(V), which resembles the high-pH form of *E. coli* nitrate reductase. The Mo(V) detected by EPR was absent from a mutant which does not assemble the molybdenum cofactor. In these cases, the levels of EPR-detectable iron–sulfur clusters in the cells were increased. Extracts from HB101/pDMS159 enriched in DmsA showed more Mo(V) signals and considerably less iron–sulfur. These results are in agreement with predictions from amino acid sequence comparisons, that the molybdenum center is located in DmsA, while four iron–sulfur clusters are in DmsB. The midpoint potentials of the molybdenum and iron–sulfur clusters in the various preparations were determined by mediator titrations. The iron–sulfur signals could be best fitted by four clusters, with midpoint potentials spread between −50 and −330 mV. The midpoint potentials of the iron–sulfur clusters and Mo(V) species were pH dependent. In addition, all potentials became less negative in the presence of the detergent Triton X-100. Observation of relaxation enhancement of the Mo(V) species by the reduced [4Fe–4S] clusters indicated that the centers are in proximity within the protein.

Dimethyl sulfoxide (DMSO)[1] reductase is a membrane-associated terminal electron transfer enzyme induced by anaerobic growth of *Escherichia coli* on fumarate-containing medium (Bilous & Weiner, 1985a,b). The expression of the enzyme is dependent on anaerobiosis and molybdenum, but not on the presence of DMSO or TMAO (Bilous & Weiner, 1985b; Cotter & Gunsalus, 1989). It reduces a broad array of *S*- and *N*-oxide compounds. Unlike the TMAO/DMSO reductase of photosynthetic bacteria, which contains molybdenum as the only cofactor (Satoh & Kurihara, 1987), the *E. coli* enzyme is a complex iron–sulfur molybdoprotein. It is composed of three nonidentical subunits (Weiner et al., 1988; Bilous et al., 1988).

We have cloned and mapped the *dms* operon to the 20′ point on the *E. coli* chromosome and sequenced the *dms* operon (Bilous et al., 1988). DMSO reductase can be expressed to high levels in cells harboring this operon on a multicopy plasmid vector. The enzyme contains the molybdenum cofactor molybdopterin, and we have shown that the membrane-extrinsic, DmsA subunit is homologous to other prokaryotic molybdopterin-containing proteins, suggesting that the cofactor is bound to this subunit (Bilous et al., 1988). The inferred amino acid sequence of DmsB indicated the presence of 16 cysteine residues organized in 4 clusters bearing homology to the iron–sulfur center binding clusters of the ferredoxins (Bruschi & Guerlesquin, 1988). DmsC is a very hydrophobic polypeptide which anchors the other two subunits to the membranes, stabilizes the catalytic subunits, and is necessary for quinol oxidase activity (J. H. Weiner, D. Sambasivarao, G. Shaw, and D. MacIsaac, unpublished experiments).

In this paper, we have used electron paramagnetic resonance to identify the iron–sulfur clusters and to characterize the redox properties of these clusters and the molybdopterin cofactor.

## Materials and Methods

*Preparation of Membrane Fraction.* *E. coli* HB101/pDMS159 was grown anaerobically on minimal glycerol/fumarate medium (Spencer & Guest, 1974) for 48 h at 37 °C. The plasmid pDMS159 carries the entire DMSO reductase operon in the vector pBR322 and has been described previously (Bilous & Weiner, 1988). In some experiments, *E. coli* F36 carrying pDMS159 was used. This strain is a mutant of HB101 in which molybdopterin insertion into DMSO reductase is impaired. This strain produces large amounts of the molybdopterin-free apoenzyme (J. H. Weiner, D. Sambasivarao, P. T. Bilous, and R. Cammack, unpublished experiments). Cells were harvested, washed, and lysed by passage through a French pressure cell as described previously (Bilous & Weiner, 1985a; Lemire et al., 1983). Membranes were isolated by centrifugation for 90 min at 150000 rpm in a Beckman Ti50.2 rotor. Crude membranes were resuspended in a minimal volume of 0.1 M MOPS buffer, pH 7.0, containing 2 mM phenylmethanesulfonyl fluoride. The supernatant fraction containing the cytoplasm either was used di-

† This work was funded by a grant from the Medical Research Council of Canada to J.H.W. (MT5838). R.C. received a Visiting Scientist award from the Alberta Heritage Foundation for Medical Research.

* Author to whom correspondence should be addressed.
‡ King's College, London.
§ University of Alberta.

[1] Abbreviations: DMSO, dimethyl sulfoxide; EPR, electron paramagnetic resonance; TMAO, trimethylamine *N*-oxide.

0006-2960/90/0429-8410$02.50/0 

Table I: Purification of DMSO Reductase to Yield the "Sephacryl Form"[a]

| fraction | units | protein (mg/mL) | sp act. (units/mg) | x-fold purification | % yield |
|---|---|---|---|---|---|
| membranes | 38799 | 341 | 113.4 | | 100 |
| Triton extract | 31000 | 180.5 | 171.8 | 1.5 | 80 |
| DE52 pool | 26350 | 39.3 | 669 | 5.9 | 68 |
| S300 | 16073 | 21.84 | 736 | 6.5 | 41 |

[a] Activity was measured with 70 mM TMAO as substrate.

rectly or used after concentration in an Amicon ultrafiltration apparatus equipped with a PM30 membrane.

*Purification of DMSO Reductase.* Twenty-six grams wet weight of *E. coli* HB101/pDMS159 grown anaerobically for 48 h in a minimal glycerol/fumarate medium (Spencer & Guest, 1974) was washed with 260 mL of 30 mM Tris-HCl, pH 8.0, resuspended in 75 mL of 200 mM potassium phosphate, pH 6.8, containing 2 mM PMSF, 10 μg/mL DNase, 10 μg/mL RNase, and 40 mM $MgCl_2$, and passed twice through a French pressure cell at 16000 psi. The lysate was spun for 10 min, 4 °C at 10000 rpm, in a Beckman JA20 rotor and the supernatant spun for 60 min, 4 °C at 40000 rpm, in a Beckman Ti50.2 rotor. The membrane pellet was resuspended in a final volume of 8.8 mL of histidine buffer (20 mM histidine, pH 6.8, 10% glycerol, 0.5 mM EDTA, and 0.5 mM DTT). Seven milliliters of the resuspended membranes (38.8 mg/mL) was diluted to 21 mg/mL in protein with histidine buffer and extracted with Triton X-100 at a detergent to protein ratio of 0.8 (217 mg of Triton X-100) and incubated at 4 °C for 30 min with occasional mixing. The extract was centrifuged at 40000 rpm for 60 min at 4 °C in the Ti50.2 rotor. The supernatant was applied to a 65-mL DE-52 column (3 × 8.8 cm) equilibrated in histidine buffer containing 0.1% Triton X-100. The column was eluted at 1 mL/min with a linear gradient from 0 to 400 mM KCl in histidine buffer plus Triton X-100. Activity eluted near the middle of the gradient. Active fractions were pooled, concentrated with an Amicon ultrafiltration cell equipped with a PM30 membrane, and applied to a 700-mL Sephacryl S-300 HR column (3.2 × 85 cm) equilibrated in histidine buffer plus 0.1% Triton X-100 and 200 mM KCl. The column was eluted at 2 mL/min, and the active fractions were pooled and concentrated as above and stored in small aliquots at −70 °C. This enzyme had a specific activity of 736 units/mg using TMAO as substrate. The purification is summarized in Table I.

This enzyme is termed the "Sephacryl form" of DMSO reductase and was compared with the "IEF form" holoenzyme prepared by chromatofocusing and DEAE-cellulose chromatography as previously described (Weiner et al., 1988) which had a specific activity of 780 units/mg with TMAO as substrate.

Triton X-100 extracts of the membranes were prepared by adding a 10% w/v solution of Triton X-100 to 0.8 mg/mg of protein and incubating for 1 h at 4 °C followed by centrifugation at 150000 rpm for 90 min at 4 °C.

DmsAB dimer was isolated as previously described (Weiner et al., 1988) from the detergent-free KCl wash of the DEAE-cellulose column prior to elution of the holoenzyme.

DmsA was found in high concentration in the cytoplasmic fraction of HB101/pDMS159 after removal of the membranes. This fraction was concentrated by ultrafiltration and chromatographed on a 700-mL Sepharose S300 HR column (3.2 × 85 cm) equilibrated with 20 mM histidine, pH 6.8, 10% glycerol, 0.5 mM EDTA, 0.5 mM DTT, and 200 mM KCl. Peak fractions were pooled, concentrated, and used directly for EPR studies. This fraction lacked detectable DmsB by Coomassie blue staining of polyacrylamide gels (Laemmli, 1970), but small amounts of DmsB could be detected by immunoblotting (Broome & Gilbert, 1978).

*Assay of DMSO/TMAO Reductase Activity.* DMSO reductase was assayed by using the TMAO- or DMSO-dependent oxidation of reduced benzyl viologen as described previously (Bilous & Weiner, 1985a) except that 50 mM MOPS buffer, pH 7.0, was used in place of 0.2 M potassium phosphate. This results in a 10–12-fold enhancement of activity compared to phosphate buffer; 70 mM TMAO was routinely used as substrate as it gave a 3.5-fold greater rate than DMSO. One unit corresponds to 1 μmol of benzyl viologen oxidized per minute. The specific activity of the membranes used for EPR studies was 113 units/mg, measured with TMAO as substrate.

*EPR Spectroscopy.* EPR spectra were recorded on a Bruker ESP300 spectrometer equipped with an Oxford Instruments ESR900 helium flow cryostat. Integrations were performed by double integration with Cu(II)–EDTA as standard. The magnetic field was calibrated relative to diphenylpicrylhydrazyl and manganese in SrO standards. Microwave power saturation data were plotted and fitted to an empirical equation as described by Rupp et al. (1978).

*Preparation of EPR Samples Poised at Defined Redox Potentials.* Samples were placed in an anaerobic chamber similar to that described by Dutton (1978), under argon, in 0.1 M MOPS buffer, pH 7.0. Mediators added, in the appropriate regions of potential, were 2,6-dichloroindophenol, phenazine methosulfate, thionine, methylene blue, resorufin, indigodisulfonate, naphthalene-1,5-disulfonate, anthraquinone-1,5-disulfonate, safranin T, benzyl viologen, and methyl viologen, all at 40 μM. The redox potential was measured with a platinum and calomel electrode, at 25 °C. The potential was adjusted with small additions of 0.1 M dithionite and 0.2 M ferricyanide solutions. After an equilibration time, at least 2 min, samples were transferred with a microliter syringe through an anaerobic chamber (Chamorovosky & Cammack, 1982) into quartz tubes and frozen in liquid nitrogen. Potentials are recorded relative to the standard hydrogen electrode.

## Results

*EPR Signals from Iron–Sulfur Clusters in the Membrane-Bound State.* Membranes from HB101/pDMS159, which overproduces DMSO reductase, were used in these studies. The only other iron–sulfur protein known to be present in the membranes was fumarate reductase, traces of which are shown as a signal with an upward feature at $g = 2.03$, crossing the base line at $g = 2.01$ (Figure 1a). This signal, observed in the oxidized state at temperatures below 30 K, is characteristic of a [3Fe–4S] cluster and is assigned to center 3 (Johnson et al., 1985a; Cammack et al., 1986). Also visible in Figure 1a is a minor signal due to molybdenum, which is saturated with microwave power under the conditions of measurement.

The iron–sulfur clusters in the membranes were reduced by dithionite within 1 min. The EPR spectrum of the reduced membranes, measured at temperatures above 40 K, showed a minor signal at $g = 1.94$ (not shown), which we attribute to fumarate reductase center 1 (Cammack et al., 1986). At temperatures below 40 K, a broad and complex feature around $g = 1.94$ was observed (Figure 1b). In the membranes from *E. coli* strain HB101/pDMS159, this spectrum was much more intense than that of fumarate reductase and is attributed to DMSO reductase. All of the spectra of the iron–sulfur

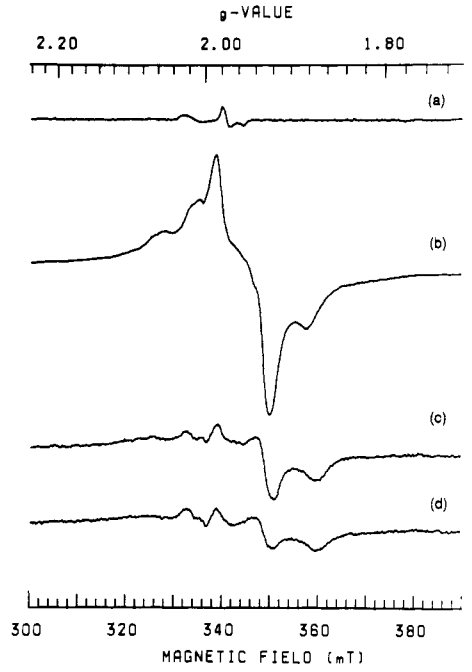


FIGURE 1: Spectra of pDMS159 membranes, measured at 12 K, showing the signals of reduced iron–sulfur clusters. Conditions of measurement were the following: microwave power, 20 mW; frequency, 9.42 GHz; modulation amplitude, 1 mT; modulation frequency, 100 kHz; receiver gain, $10^5$. (a) Oxidized as prepared; (b) treated with 2.5 mM dithionite; (c) treated with 2.5 mM dithionite plus 25 mM TMAO; (d) treated with 2.5 mM dithionite plus 25 mM DMSO. Samples were treated for 1 min at 20 °C prior to freezing.

clusters in DMSO reductase were most clearly resolved at temperatures around 12 K and completely broadened out at 40 K. This temperature dependence is indicative of reduced [4Fe–4S] clusters.

Addition of excess DMSO or TMAO to the dithionite-reduced membranes caused a substantial reoxidation of the iron–sulfur clusters. Only a small rhombic EPR signal from one reduced iron–sulfur cluster remained (Figure 1c,d). Dithionite is a very poor reducing substrate for the enzyme, and a steady state would be set up in these samples in which the state of oxidation of the enzyme was largely determined by the DMSO/DMS or TMAO/trimethylamine couples (160 and 130 mV, respectively). This observation shows that most, if not all, of the EPR-detectable iron–sulfur clusters have more negative midpoint potentials.

When the membranes were extracted with Triton X-100, the EPR signals of the soluble extracts were similar to those of the membrane-bound DMSO reductase. Solubilization did not appear to affect the spectroscopic properties of the iron–sulfur clusters in the protein significantly. The same was found to be true of the EPR spectra of the molybdenum center, although the midpoint potentials were somewhat less negative than in the membranes.

*EPR Signals of the Iron–Sulfur Clusters in the Purified Enzyme.* Figure 2A shows the iron–sulfur signals of the "IEF form" of holoenzyme, and Figure 2B shows the iron–sulfur signals of the "Sephacryl form" of holoenzyme containing DmsA, -B, and -C. The latter form gave similar iron–sulfur signals to the membrane-bound enzyme (compare Figure 2B with Figure 1b). The integrated intensity of the spectrum around $g = 1.94$, after correction for microwave power saturation, corresponds to $3.82 \pm 0.5$ spins per molecule. The main differences from the membrane-bound enzyme are in the relative intensities of the molybdenum and iron–sulfur signals (see below). The molybdenum intensity was considerably

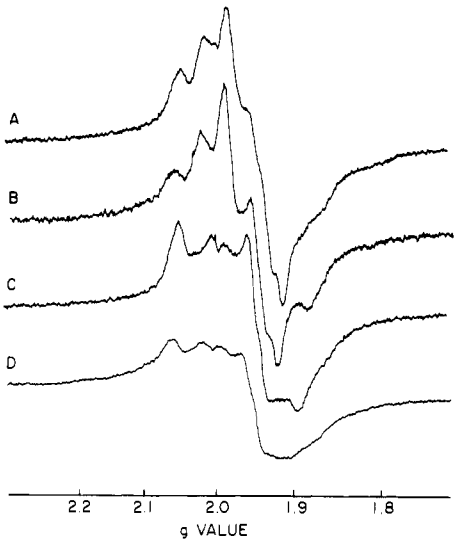


FIGURE 2: Comparison of the EPR spectra of iron–sulfur clusters in (A) purified DMSO reductase "IEF form", (B) purified DMSO reductase "Sephacryl form", (C) DmsAB dimer, and (D) enriched DmsA. Gain settings are arbitrary. Spectra were recorded at 12 K with microwave power 20 mW, frequency 9.42 GHz.

higher, particularly in the IEF form of enzyme prepared by isoelectric focusing.

The fraction enriched in the DmsAB dimer (Figure 2C) also showed typical iron–sulfur cluster signals on reduction with dithionite. The spectrum had a somewhat different line shape, indicating a different conformation of the protein or the absence of certain clusters. The iron–sulfur clusters were reoxidized by DMSO and TMAO in a similar way to the membrane-bound protein (data not shown). Thus, DmsC does not seem to be necessary for interaction of the iron–sulfur clusters with the oxidizing substrates.

The cytoplasm of strains of *E. coli* overproducing DMSO reductase is enriched in soluble DmsA. Although DmsB could not be detected in soluble extracts by protein staining, small amounts of DmsB were observed by immunoblotting (Broome & Gilbert, 1978). This soluble DmsA-enriched fraction obtained from the cytoplasm (Figure 2D) showed EPR signals from iron–sulfur clusters which were qualitatively similar to those of the protein in the membrane, but quantitatively about 5-fold less, in comparison with the molybdenum signals (see below). This is consistent with the conclusion that the DmsA subunit contains the molybdenum center, if it is assumed that this preparation was contaminated with about 20% of the iron–sulfur protein DmsB.

*Redox Potentials of the Iron–Sulfur Centers.* In a titration of the purified protein at controlled redox potentials, at pH 7, reduction of the iron–sulfur clusters could be observed by EPR spectroscopy. This was most clearly seen (Figure 3) in membranes from mutant *E. coli* F-36 in which the spectra were free from overlapping molybdenum signals. Similar behavior was observed in all the membrane-bound preparations and in the "Sephacryl form" of enzyme.

Several types of iron–sulfur signals could be resolved as the enzyme was progressively reduced. First, a rhombic EPR signal was observed, at $g = 2.01$, 1.93, and 1.866. This is similar to the spectrum of the DMSO-reoxidized sample of DMSO reductase (compare Figure 3a with Figure 1d). This is assigned to the cluster with the most positive midpoint potential, which we refer to as cluster 1. Second, at potentials around −60 to −100 mV, a more complex signal appeared with a feature around $g = 2$, indicating the reduction of another iron–sulfur cluster or clusters. At this stage, the amplitude

Table II: Midpoint Potentials of Centers in Different Preparations[a]

| preparation | pH | Mo | | | Fe-S | | | |
|---|---|---|---|---|---|---|---|---|
| | | VI/V | V/IV | mid | 1 | 2 | 3 | 4 |
| pDMS159 membranes | 7.0 | −75 | −90 | −83 | −50 | −120 | −240 | −330 |
| pDMS159 membranes | 9.0 | −125 | −120 | −123 | −90 | −250 | −330 | −400 |
| Triton X-100 extract | 7.0 | 15 | −100 | −43 | −25 | −130 | −250 | −340 |
| Triton X-100 extract | 5.5 | 65 | 35 | 50 | 20 | −60 | −170 | −265 |
| F-36 membranes | 6.8 | | | | −60 | −130 | −240 | −340 |
| purified DMSO reductase, "Sephacryl form" | 7.0 | 45 | −150 | −53 | −50 | −120 | −230 | −330 |
| DmsA | 7.0 | 50 | −100 | −25 | | | | |

[a] Potentials are in millivolts vs SHE.

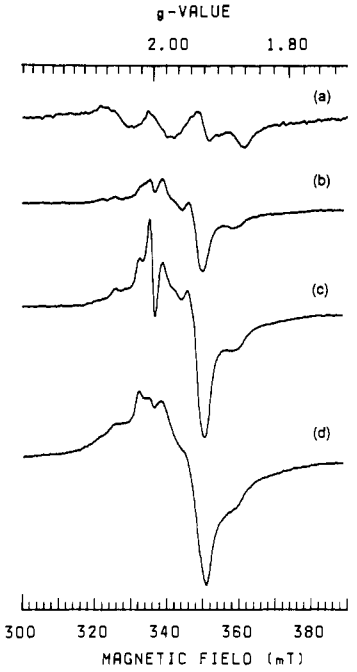


FIGURE 3: EPR spectra from membranes of *E. coli* F-36, showing the signals due to iron–sulfur clusters. The samples were poised at (a) −51, (b) −157, and (c) −359 mV; (d) is a sample without mediators, reduced with dithionite. Spectra were recorded at 12 K with a microwave power of 20 mW, a frequency of 9.2 GHz, and a modulation amplitude of 0.2 mT.

of the extreme high-field feature of cluster 1 at $g = 1.866$ decreased (Figure 3b). This behavior is similar to that in the 2[4Fe–4S] ferredoxins (Mathews et al., 1974); it arises because of the spin–spin interactions between two iron–sulfur clusters in the protein. The spectrum of the interacting pair of clusters lacks some of the features of the spectra of the individual clusters.

During the final reduction, between −200 and −400 mV, the spectrum continued to increase; further spectra appeared around $g = 1.94$, with additional features to low field at $g = 2.06$, and in the center of the spectrum at $g = 2.02$ and $g = 1.98$ (Figure 3c,d). At the lowest potentials, broad outer lines appeared. The broadness is presumably due to spin–spin interactions between adjacent iron–sulfur clusters.

An indication of the increase in iron–sulfur cluster signal intensity on reduction is provided by the amplitude of the $g = 1.94$ signal. In Figure 4, the derivative amplitude, measured from the upward feature at $g = 1.94$ to the downward feature at $g = 1.92$, is plotted as a function of applied redox potential, for the membrane-bound DMSO reductase. The reduction pattern for the "Sephacryl form" DMSO reductase was similar to that in membranes (Figure 5, closed diamonds). However, in the "IEF form" of DMSO reductase, purified by the previously published method using isoelectric focusing, the amount of the two lower potential waves in the titration curves was

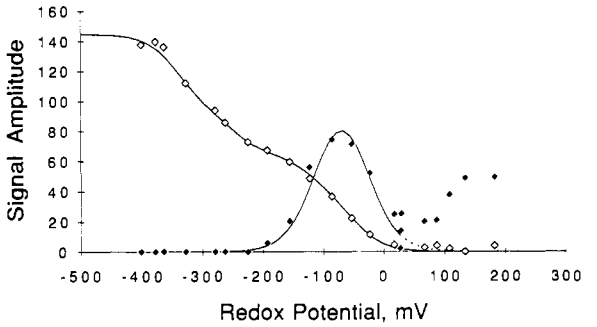


FIGURE 4: Redox titration curves showing the changes in the amplitude of the $g = 1.94$ signal due to iron–sulfur clusters, recorded at 12 K (◇), and the $g = 1.98$ signal due to molybdenum, recorded at 120 K (◆). Signals were measured as for Figures 3 and 7, respectively.

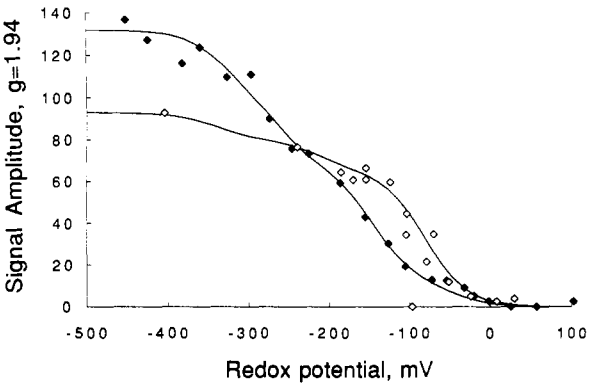


FIGURE 5: Amplitude vs applied redox potentials for the $g = 1.94$ signals in DMSO reductase prepared (◇) "IEF form" (4) and (◆) "Sephacryl form", as described in the text.

considerably decreased (Figure 5, open diamonds), indicating that selective destruction of the low-potential iron–sulfur clusters had taken place.

Midpoint potentials derived from titrations of the purified enzyme, and of the other fractions of DMSO reductase under various conditions, are presented in Table II. The pH dependence of the redox potentials of the iron–sulfur clusters showed that the midpoint potentials shifted slightly with pH, becoming more negative at pH 9 and less negative at pH 5.

*EPR Signals Due to Molybdenum.* In the membranes isolated from the DMSO reductase enriched cells, an EPR signal was observed with rhombic symmetry at $g = 1.987$, 1.976, and 1.960 (Figure 6), at temperatures higher than those required for the iron–sulfur cluster signals (120 K). This spectrum is similar to the spectrum of the high-pH form of Mo(V) in *E. coli* nitrate reductase (Vincent & Bray, 1978). It was observed in preparations from pH 5 to pH 9.

The Mo(V) signal was stable as long as the membranes remained oxidized. On progressive reduction to more negative potentials (100 mV), the signal decreased at first (Figure 4, closed diamonds) and if reoxidized at this stage, it did not reappear. During further reduction, the signal reappeared,

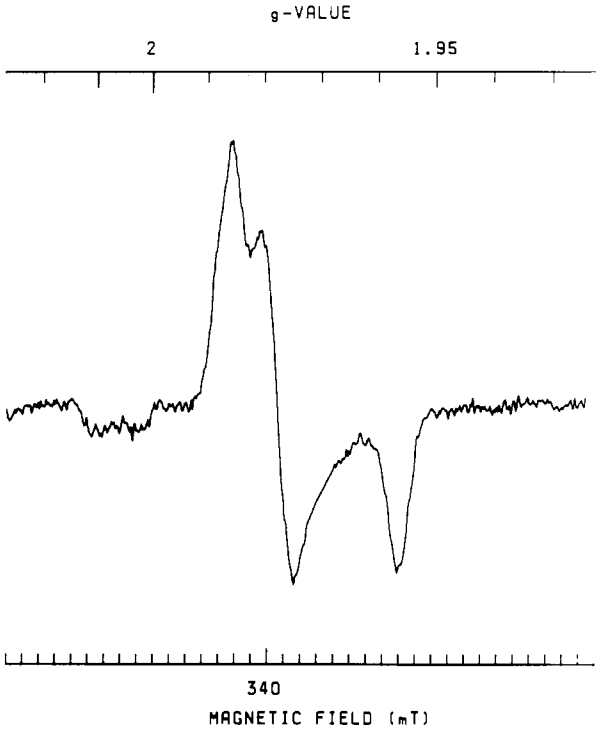


FIGURE 6: EPR spectrum of molybdenum in purified DMSO reductase "Sephacryl form", poised at a potential of −51 mV. The spectrum was recorded at 120 K, with a microwave power of 20 mW, a frequency of 9.42 GHz, and a modulation amplitude of 0.2 mT.

reaching a maximum at about −55 to −75 mV, and then decreased to zero. The redox behavior in this region of potential, which was completely reversible, is as expected for Mo(V), which is an intermediate redox state between the diagmagnetic states Mo(VI) and Mo(IV). The potential for the maximum signal intensity corresponds to the average of the midpoint potentials of the Mo(VI)/Mo(V) and Mo(V)/Mo(IV) couples. This can be estimated with considerable accuracy (±15 mV). In order to estimate the individual midpoint potentials, it was necessary to estimate the intensity of the Mo(V) signals relative to the concentration of active enzyme. The intensity of the molybdenum concentration was determined by numerical double integration of spectra recorded at 120 K under non-saturating conditions. Since the preparations of the enzyme were not homogeneous, its concentration was estimated from the intensity of the iron–sulfur signals in the fully reduced protein, with corrections for microwave power saturation, different temperatures and instrument settings, and the percentage of molybdenum isotopes with zero nuclear spin. For these purposes, the enzyme was assumed to contain four iron–sulfur clusters per molecule. As a consequence of the combined errors in spin concentrations, the uncertainty in the midpoint potentials is larger, ±40 mV. Another factor which can affect the reliability of these estimates is the possibility of redistribution of electrons within the enzyme molecule during freezing. It has been observed in xanthine oxidase that the potentials determined at cryogenic temperatures differ from those measured at room temperature, though the effect is less in zwitterionic buffers [reviewed in Hille and Massey (1978)].

The midpoint potentials of the molybdenum signals of various preparations are listed in Table II. The midpoint potentials of the iron–sulfur clusters and molybdenum in the membrane-bound enzyme were pH dependent. When measured in the membranes, they were more negative at pH 9. Measurements at pH of 6 or less were made on extracts in Triton X-100, to avoid coagulation. It can be seen that

Table III: Relative Signal Intensities of EPR Signals in Different Preparations

| preparation | pH | max signal intensity (nmol/mg of protein) Fe–S | Mo |
|---|---|---|---|
| pDMS159 membranes | 7.0 | 1.80 | 0.11 |
| pDMS159 TX-100 extract | 7.0 | 2.92 | 0.19 |
| F-36 membranes | 6.8 | 6.82 | 0 |
| purified DMSO reductase | 7.0 | 27.2 | 5.4 |
| DmsA | 7.0 | 1.51 | 0.45 |

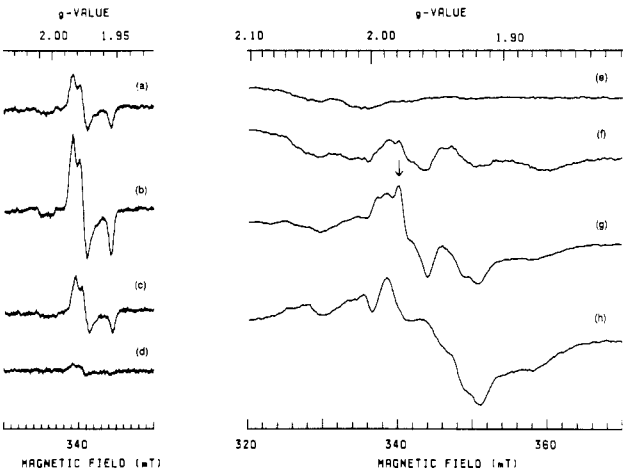


FIGURE 7: Spectra of purified DMSO reductase "Sephacryl form" during reductive titration. (a and e) +175 mV; (b and f) −51 mV; (c and g) −154 mV; (d and h) −239 mV. Spectra a–d were recorded at 120 K and show the signal of Mo(V). Spectra e–h were recorded at 12 K and show the signals for iron–sulfur, with the feature assigned to Mo(V) marked with an arrow.

treatment with Triton at pH 7.0 caused positive shifts in the midpoint potentials relative to the membrane-bound form (the potentials of the purified enzyme, which also contained this detergent, were similarly shifted). The midpoint potentials of the molybdenum in particular became significantly more positive at pH 5.5.

The intensities of the signals of iron–sulfur clusters and molybdenum are summarized in Table III. The intensities of the Mo(V) signals presented are the maxima observed in the reductive titrations, and are a function of both the amounts of molybdenum present and the relative Mo(VI)/Mo(V) and Mo(V)/Mo(IV) couples. The preparations enriched in soluble DmsA showed spectra due to molybdenum with maximum intensity at −25 mV, somewhat less negative than the molybdenum in the membrane-bound protein. The small signals from iron–sulfur clusters probably represent residual DmsB. No molybdenum signals were detected in membranes from *E. coli* mutant F-36/pDMS159.

In the "IEF form" of purified DMSO reductase, the potentials for the Mo(VI)/Mo(V) and Mo(V)/Mo(IV) couples were more widely separated than in the membranes. This indicates that the Mo(V) species is more stable in this form of the enzyme, which may indicate some modification of the protein during purification.

The Mo(V) signal in DMSO reductase, which in the isolated state was strongly saturated with microwave power, became extremely rapidly relaxing in the presence of reduced iron–sulfur clusters. This is demonstrated by three different lines of evidence:

(1) The EPR spectrum of molybdenum, which was normally strongly saturated by 20-mW microwave power at a temperature of 12 K (see Figure 1a), appeared quite prominently in some samples of the purified enzyme at poised potentials.

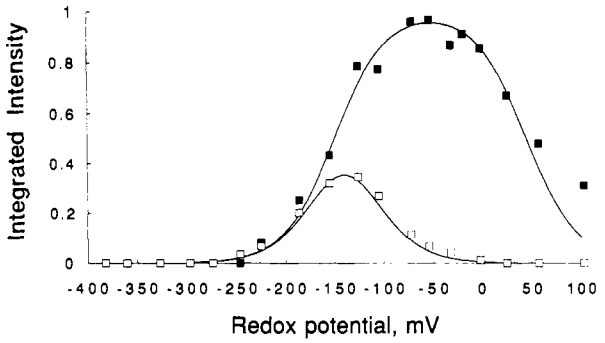


FIGURE 8: Plots of the integrated intensity of the Mo(V) spectrum against the applied redox potential. Spectra were recorded at 20-mW microwave power (■) at 120 K and (□) at 30 K.

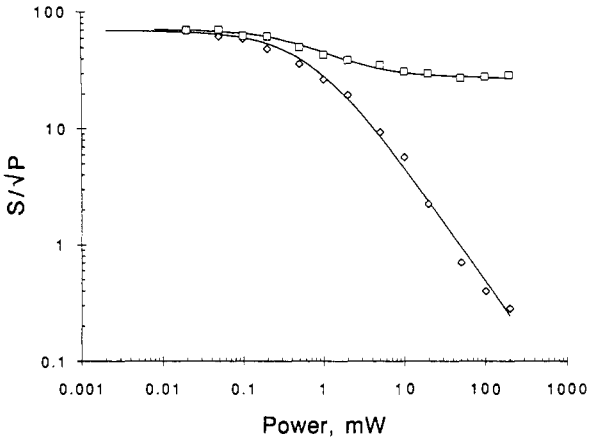


FIGURE 9: Power saturation curves of Mo(V) signals, measured at 30 K. Sample poised at (◇) −20 and (□) −155 mV.

The signal is shown arrowed in Figure 7g, superimposed on the spectra of the iron–sulfur clusters which are expanded for clarity. This signal is assigned to molybdenum on the basis that it was not observed in the mutant F-36. In Figure 7, the amplitude of the Mo(V) species, measured under nonsaturating conditions (a–d) is compared with the amplitude in the same samples measured at 12 K (e–h). It can be seen that the $g = 1.98$ signal was maximal at potentials where the iron–sulfur clusters were significantly reduced (spectrum g), although this potential was not the optimum for Mo(V), The appearance of the molybdenum signal at low temperatures may be attributed to a spin–spin interaction between the molybdenum and an iron–sulfur cluster.

(2) The Mo(V) signal measured a saturating microwave power and 30 K (Figure 8) shows a different redox potential profile from the molybdenum signal measured under nonsaturating conditions at 120 K. The saturated signal indicates a lower apparent midpoint potential. This can be explained on the basis that the amplitude of the signal depends on the probability of *both* the molybdenum *and* the iron–sulfur center being simultaneously paramagnetic in the same enzyme molecule. In Figure 8, the shape of the titration curve was fitted on the assumption that the molybdenum interacts with a single redox center of midpoint potential −120 mV.

(3) Microwave power saturation curves of the molybdenum EPR spectrum at 30 K (Figure 9) show that the power for half-saturation of the normal Mo(V) signal, in a sample where the iron–sulfur clusters were mostly oxidized, was less than 1 mW. In a sample where a substantial amount of Fe–S clusters 1 and 2 was reduced, a significant fraction of the Mo(V) signal was very rapidly relaxing at this temperature. The data could be fitted to two components, one relaxing like the Mo(V) in the first sample and one which was not significantly saturated even at a microwave power of 200 mW. As expected, the fraction of the total Mo(V) signal which was rapidly relaxing increased at lower redox potentials where a higher proportion of iron–sulfur clusters was reduced.

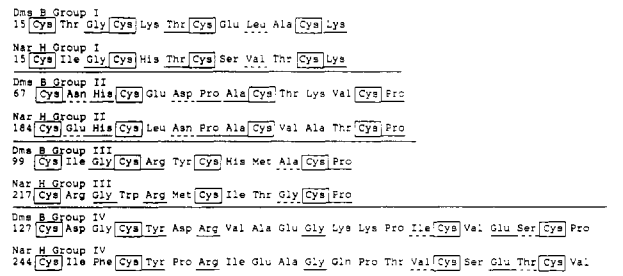


FIGURE 10: Sequence of the cysteine clusters in DMSO reductase (DmsB) and nitrate reductase NarH. The sequence for DMSO reductase is taken from Bilous et al. (1988). The nitrate reductase sequence was provided by Blasco et al. (1989).

## Discussion

On the basis of analysis of the inferred DNA sequence of DMSO reductase, we suggested that the 16 Cys residues in DmsB were arranged in 4 groups which could ligate iron–sulfur centers (Bilous et al., 1988), and these are shown in Figure 10. In agreement with this, we find that the EPR spectrum of the reduced reductase, both in the membrane-bound state and in the purified state, can best be fitted by four Fe–S signals. These clusters are referred to as centers 1–4, in order of decreasing potential. It is not known which cysteines in the sequence bind to which of the clusters. The sequences of [4Fe–4S] ferredoxins show a cluster binding motif consisting of three cysteines, arranged like the first three cysteines in each of groups I–IV (Figure 10), and a fourth distant cysteine (usually Cys–Pro) from another group.

Comparison of DmsB with the NarH sequence coding for the iron–sulfur-containing subunit of nitrate reductase (Blasco et al., 1989) indicates that the organization of the Cys residues is highly conserved in both proteins (Figure 10) except that NarH codes for only 15 Cys. In the third group of cysteines, the second Cys residue is replaced by a Trp. In proteins such as ferredoxin I from *Azotobacter vinelandii* (Stout et al., 1988), ferredoxin II from *Desulfovibrio gigas* (Kissinger et al., 1989), and probably also fumarate reductase (Johnson et al., 1985a), such an arrangement of three cysteines will coordinate to a [3Fe–4S] cluster. It is significant that oxidized nitrate reductase shows a strong EPR signal in the oxidized state (DerVartanian & Forget, 1975), with a midpoint potential of +80 mV (Vincent, 1979) which has been assigned to a [3Fe–4S] cluster (Johnson et al., 1985b). No iron–sulfur signals were detected in oxidized DMSO reductase, which presumably has a [4Fe–4S] cluster in the same position.

The midpoint potentials of the glycerol 3-phosphate/dihydroxyacetone phosphate and DMSO/DMS couples, which are the physiological electron donor and acceptor, are −290 mV and +160 mV, respectively. All of the iron–sulfur clusters in DMSO reductase are therefore competent to transfer electrons between these couples, but apparently only clusters 1 and 2 are well placed to accept electrons from the intermediate carrier menaquinol (−80 mV). The potentials of clusters 3 and 4 are more negative, like typical [4Fe–4S] bacterial ferredoxins (Cammack, 1984), and their function, like center 2 of fumarate reductase (Cammack et al., 1986), is unclear.

The DMSO reductase prepared by Sephacryl gel filtration has a much higher specific activity with quinones as donors (1400 nmol of dimethylnaphthoquinol oxidized $min^{-1}$ $mg^{-1}$)

than the enzyme prepared by isoelectric focusing (215 nmol $min^{-1}$ $mg^{-1}$) (J. H. Weiner, D. Sambasivarao, G. Shaw, and D. MacIsaac, unpublished experiments). Moreover, while the iron–sulfur EPR signals of the "Sephacryl form" were similar to those in membranes (Figure 5), the "IEF form" was deficient in the low-potential iron–sulfur clusters. This may be due to destruction of the iron–sulfur clusters at acid pH.

DMSO reductase has been shown to be a molybdenum-containing enzyme, both by direct Mo analysis and by comparison of the inferred amino acid sequence of DmsA with other prokaryotic molybdopterin-containing enzymes (Bilous et al., 1988), and now by EPR analysis. The midpoint potentials of the Mo(VI)/(V) and Mo(V)/(IV) transitions lie between the potential of the iron–sulfur clusters and that of the DMSO/dimethyl sulfide couple. The potentials are more negative than those in nitrate reductase, which were estimated to be +220 and +180 mV for the Mo(VI)/Mo(V) and Mo(V)/Mo(IV) (low-pH form), respectively, and +50 mV for one of the iron–sulfur clusters (Vincent, 1979). The similarity of the Mo(V) spectrum in DMSO reductase to that of the high-pH form of nitrate reductase (Vincent & Bray, 1978) indicates a similar ligand geometry.

The molybdenum center in DMSO reductase enriched membranes, prepared under air, was observed to be partially in the paramagnetic Mo(V) state. This is despite the fact that the molybdenum redox potentials are less than 0 mV. After reduction and reoxidation in the presence of mediator dyes, the Mo(V) signal disappeared. A similar Mo(V) signal was observed in freshly prepared nitrate reductase (Vincent & Bray, 1978). The presence of this Mo(V) state may be explained by assuming that, after oxidation, a fraction of the enzyme contains a single electron per molecule. The molybdenum center, being the highest potential component, would remain as the paramagnetic Mo(V), which could not react with two-electron acceptors such as DMSO.

The observed spin–spin interactions between molybdenum and at least one of the iron–sulfur clusters show that the redox centers are in proximity, even though they are on different subunits, DmsA and -B, respectively. Interactions between iron–sulfur clusters 1 and 2, and between cluster 4 and some of the other clusters, are indicated by the changes in line shape of the signals during progressive reduction of the protein (Figure 3). Completely reduced enzyme is characterized by broad outer lines, as in dithionite-reduced nitrate reductase from *E. coli* (Johnson et al., 1985b). Similar EPR spectra with broad outer lines are also observed in ferredoxins with two reduced [4Fe–4S] clusters, where the distance between the clusters in the ferredoxins is about 12 Å (Mathews et al., 1974). It was not possible to estimate the distance between the molybdenum and the iron–sulfur clusters, as was done in the case of xanthine oxidase (Barber et al., 1982), because the power for half-saturation of the molybdenum was too high to be estimated. However, the large spin–spin relaxation enhancement effect of the molybdenum spectrum, and the lack of significant dipolar broadening, indicates that the distance between the Mo(V) and iron–sulfur cluster 2 is between 12 and 8 Å (Coffman & Buettner, 1979).

## Acknowledgments

We thank Dr. Alan Chapman, Gillian Shaw, and Doug MacIsaac for assistance with enzyme preparations and spectroscopy and the staff of the University of Alberta Departments of Chemistry, Physics, and Physiology for their willing provision of apparatus and space during these studies.

**Registry No.** Mo, 7439-98-7; DMSO reductase, 73200-91-6.

## References

Barber, M. J., Salerno, J. C., & Siegel, L. M. (1982) *Biochemistry 21*, 1648–1656.

Bilous, P. T., & Weiner, J. H. (1985a) *J. Bacteriol. 162*, 1151–1155.

Bilous, P. T., & Weiner, J. H. (1985b) *J. Bacteriol. 163*, 369–375.

Bilous, P. T., & Weiner, J. H. (1988) *J. Bacteriol. 170*, 1511–1518.

Bilous, P. T., Cole, S. T., Anderson, W. F., & Weiner, J. H. (1988) *Mol. Microbiol. 2*, 785–795.

Blasco, F., Iobbi, C., Giordano, G., Chippaux, M., & Bonnefoy, V. (1989) *Mol. Gen. Genet. 218*, 249–256.

Broome, S., & Gilbert, W. (1978) *Proc. Natl. Acad. Sci. U.S.A. 75*, 2746–2749.

Bruschi, M., & Guerlesquin, F. (1988) *FEMS Microbiol. Rev. 54*, 155.

Cammack, R. (1984) in *Charge and Field Effects in Biosystems* (Allen, M. J., Usherwood, P. N. R., Eds.) pp 41–51, Abacus Press, Tunbridge Wells.

Cammack, R. Patil, D. S., & Weiner, J. H. (1986) *Biochim. Biophys. Acta 870*, 545–551.

Chamorovsky, S. K., & Cammack, R. (1982) *Photobiochem. Photobiophys. 4*, 195–200.

Coffman, R. E., & Buettner, G. R. (1979) *J. Phys. Chem. 83*, 2392–2400.

Cotter, P. A., & Gunsalus, R. P. (1989) *J. Bacteriol. 171*, 3817–3823.

DerVartanian, D. V., & Forget, P. (1975) *Biochim. Biophys. Acta 379*, 74–80.

Dutton, P. L. (1978) *Methods Enzymol. 54*, 411–435.

Hille, R., & Massey, V. (1985) *Met. Ions Biol. 7*, 443–518.

Johnson, M. K., Morningstar, J. E., Cecchini, G., & Ackrell, B. A. C. (1985a) *Biochem. Biophys. Res. Commun. 131*, 653–658.

Johnson, M. K., Bennett, D. E., Morningstar, J. E., Adams, M. W. W., & Mortenson, L. E. (1985b) *J. Biol. Chem. 260*, 5456–5463.

Kissinger, C. R., Adman, E. T., Sieker, L. C., Jensen, L. H., & LeGall, J. (1989) *FEBS Lett. 244*, 447–450.

Laemmli, U. K. (1970) *Nature (London) 227*, 680–685.

Lemire, B. D., Robinson, J. J., Bradley, R. D., Scraba, D. G., & Weiner, J. H. (1983) *J. Bacteriol. 155*, 391–397.

Mathews, R., Charlton, S., Sands, R. H., & Palmer, G. (1974) *J. Biol. Chem. 249*, 4326–4328.

Rupp, H., Rao, K. K., Hall, D. O., & Cammack, R. (1978) *Biochim. Biophys. Acta 537*, 255–269.

Satoh, T., & Kurihara, F. N. (1987) *J. Biochem. (Tokyo) 102*, 191–198.

Spencer, M. E., & Guest, J. R. (1974) *J. Bacteriol. 117*, 954–959.

Stout, G. H., Turley, S., Sieker, L. C., & Jensen, L. H. (1988) *Proc. Natl. Acad. Sci. U.S.A. 85*, 1020–1023.

Vincent, S. P. (1979) *Biochem. J. 177*, 757–759.

Vincent, S. P., & Bray, R. C. (1978) *Biochem. J. 171*, 639–647.

Weiner, J. H., MacIsaac, D. P., Bishop, R. E., & Bilous, P. T. (1988) *J. Bacteriol. 170*, 1505–1510.